CHAPTER VIII
Cr-MODIFIED γ-ALUMINA CATALYSTS FOR BIO-CHEMICAL PRODUCTION VIA CATALYTIC DEHYDRATION OF BIO-ETHANOL

8.1 Abstract

The catalytic dehydration of bio-ethanol is one of the most attractive routes for hydrocarbons in the gasoline range and gives high valuable oxygenate compounds as a co-product. In this work, the formation of hydrocarbons and oxygenate compounds in the catalytic dehydration of bio-ethanol was investigated using 5 wt% Cr loading of both metallic and metal oxide forms, which were prepared by using incipient wetness impregnation method, were used to examine. A 3 g of catalyst was used in the continuous fixed bed U-tube reactor at 500°C under atmospheric pressure with 0.5 h^{-1} LHSV of bio-ethanol. The catalysts were characterized using SAA, XRD, and XPS. Moreover, the products were analyzed using GC-online and GC×GC-TOF/MS in order to identify the gaseous products and hydrocarbon species, respectively. As a result, it was found that the introduction of metallic Cr and CrO_3 on alumina surface resulted in the suppression in ethylene formation, and led to the increasing of hydrocarbons in oil. Moreover, CrO_3/Al_2O_3 catalyst had higher ability to produce hydrocarbons than Cr/Al_2O_3 catalyst. Moreover, the oxygenate compounds were composed of phenol, ketone, and a trace of ether compounds Furthermore, XPS analysis indicated that metallic Cr was entirely transformed to CrO, and, in the case of metal oxide catalyst, the $Cr(OH)_3$ phase appeared on the surface after the catalytic testing.

8.2 Introduction

Nowadays, the catalytic dehydration of bio-ethanol has become more attractive route to produce hydrocarbons because of some advantages, such as low production cost, energy consumption when compared with traditional route (Takahara *et al.*, 2005), and especially, the obtained gaseous products mainly consist of ethylene (Zhang *et al.*, 2008), which can be an important intermediate to transform

to various hydrocarbon products. Additionally, oligomers (C_4-C_{20}) of ethylene are important intermediates that are able to be transformed to various chemical compounds. They have several advantages in chemical industries and our diary life. For example, C_4-C_8 can be used as co-monomers with ethylene in polymerization processes to yield branched linear-low density polyethylene, which can be used to make plastic bags. Branched C_5-C_9 can be used as gasoline booster in vehicle fuels, and C_{10} can be used as synthetic lubricant and plasticizers in polymer processing process. Moreover, C_{12}-C_{20} can be used as reactants of detergent production (Speiser *et al.,* 2005). However, the products obtained from the catalytic dehydration of bio-ethanol do not only have hydrocarbons, but also oxygenate compounds as a group of products that can be used in various applications. For examples, in Thailand, ethanol is widely used in gasohol production from gasoline in order to reduce gasoline prices. Methyl-Tertiary-Butyl-Ether (MTBE) is used as octane booster to increase octane number, resulting in more complete combustion, and 2-pentanone is used as solvent in dewaxing process, and used as cleaning agent in medical treatment.

For the past decade, chromium catalysts were widely employed in order to produce large hydrocarbons. Chen *et al.*, (2007) employed chromium catalysts in ethylene tetramerization to produce 1-octane. They found that the products obtained were in the range of unsaturated C_4-C_8, and C_6 products were methylcyclopentane, and methylenecylopentane. In addition, Aguado *et al.*, (2008) studied ethylene polymerization by using chromium-supported on SBA-15 catalyst. They found that Cr/AlSBA-15 exhibited the highest activity, and the obtained product was high density polyethylene. Calleja and co-workers (2005) studied chromium-supported on Al-MCM-41 catalysts for ethylene polymerization. The results showed that polyethylene in linear form was obtained as a major product. Moreover, they explained that the large pore size and pore volume of Al-MCM-41 support can help to promote large hydrocarbon products. Furthermore, chromium catalysts, with N-isopropyl bis(diphenylphosphino)amine (PNP) ligand, supported on Y zeolite for ethylene polymerization were studied by Shoa *et al.*, 2014. They found that the catalysts were selective to produce unsaturated C4 to polyethylene in linear form with aromatic formations. In addition, Sun *et al.*, 2014 studied chromium catalysts

with boron- and silicon-based ligand for ethylene polymerization. The results showed that the products obtained were in the range of C_4 to C_{14}, and C_6 product was 1-hexene. Moreover, the hydrocarbons were totally unsaturated aliphatic hydrocarbons.

Thus, chromium catalyst is an interesting catalyst in the catalytic dehydration of bio-ethanol because chromium catalyst has potential to produce large liner hydrocarbons, and alumina which has low acidity and large pore size may help for bigger hydrocarbon formations. Therefore, the aim of this work was to examine the formation of oxygenate compounds and hydrocarbons in the catalytic dehydration of bio-ethanol by using chromium catalyst in both metal and metal oxide forms as a promoter. Moreover, the catalysts were characterized using surface area analyzer (SAA), X-ray diffraction spectroscopy (XRD), and X-ray photoelectron spectroscopy (XPS).

8.3 Experimental

8.3.1 Catalyst Preparation

γ-Al_2O_3 (γ-Alumina) used in this work was supplied form Sigma Aldrich, Singapore. Chromium (III) nitrate hexahydrate was used as chromium precursor. A metal solution of chromium nitrate was loaded on the support using incipient wetness impregnation technique until amount of 5.0 wt% Cr loading was achieved. After impregnation, the wet catalyst was dried at 110°C overnight and then calcined at 600°C, 10°C/min for 3 hours. The calcined catalyst was pelletized, crushed, and sieved to 20-40 mesh particle. Additionally, to produce Cr/Al_2O_3 catalyst, the calcined catalyst was pretreated under H_2 atmosphere at 650°C for 2 hours.

8.3.2 Catalytic Testing

The catalytic dehydration of bio-ethanol was tested in a continuous isothermal fixed-bed U-tube reactor under atmospheric pressure at 500°C with temperature controllers for 8 hours. High purity grade bio-ethanol (99.5%) was fed by a syringe pump with carrier gas, helium, through the catalyst bed. The gaseous

producys will pass through online-GC, and the liquid products that received form the reactor were condensed in cooling unit, and separate the extracted oil out by using carbon disulfide.

8.3.3 Product Analysis

The gaseous products were analyzed by using a GC-TCD (Agilent 6890N) to determine the gas composition, and GC-FID (Agilent 6890N) was used to determine the bio-ethanol and oxygenate contents. The extracted oils were analyzed by using Gas Chromatography (Agilent technology 7890) with Time-of-Fight Mass Spectrometer (LECO, Pegasus® 4D TOF/MS) equipped with the 1st GC column was a non-polar Rtx®-5sil MS (30 m × 0.25 mm × 0.25 μm), and the 2nd GC column was an Rxi®-17 MS column (1.790 m × 0.1 mm ID ×0.1 μm) to determine the composition.

8.3.4 Catalyst Characterization

The Brunauer-Emmett-Teller (BET) technique was used to determine the specific surface area, total pore volume, and pore size of catalysts using Thermo Finnigan/Sorptomatic 1990 surface area analyzer. The pore size distribution was calculated using BJH method. The X-ray diffraction of catalysts was determined using Rigagu SmartLab® in BB/Dtex mode with CuKα radiation. The machine collected the data from 10°-80° (2θ) at 5°/min with the increment of 0.01°. X-ray Photoelectron Spectroscopy (XPS) spectra were carried out using an AXIS ULTRA^{DLD}. The system was equipped with a monochromatic Al x-ray source and hemispherical analyzer. The spectrometer was operated with the pass energy of 160 and 40 eV for wide and narrow scan, respectively. All peaks were calibrated from referring C 1s spectra located at 284.8 eV.

8.4 Results and Discussion

8.4.1 Catalyst Characterization

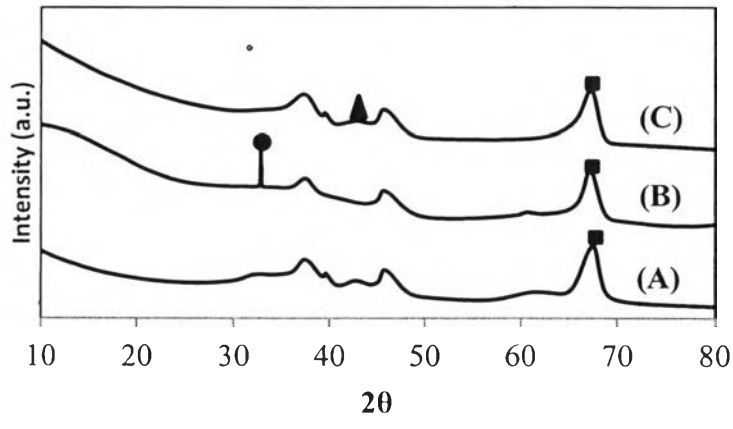

Figure 8.1 XRD patterns of (A) Al_2O_3, (B) CrO_3/Al_2O_3, and (C)Cr/Al_2O_3 (● = CrO_3, ▲ = Cr, and ■ = γ-Al_2O_3).

Table 8.1 Binding energies (eV) of chromium on fresh and spent catalysts

Sample	Phase	Cr $2p_{3/2}$		Cr $2p_{3/2}$ (sat.)		% Composition	
		Before	After	Before	After	Before	After
Cr/Al_2O_3	Cr	574.5	-	-	-	93.5	-
	CrO	-	575.2	-	-	-	85.3
	Cr_2O_3	576.1	567.4	580.3	580.6	6.5	14.7
CrO_3/Al_2O_3	Cr_2O_3	567.9	-	582.7	-	34.4	-
	CrO_3	579.6	579.7	-	-	65.6	22.3
	$Cr(OH)_3$	-	577.6	-	582.2	-	77.7

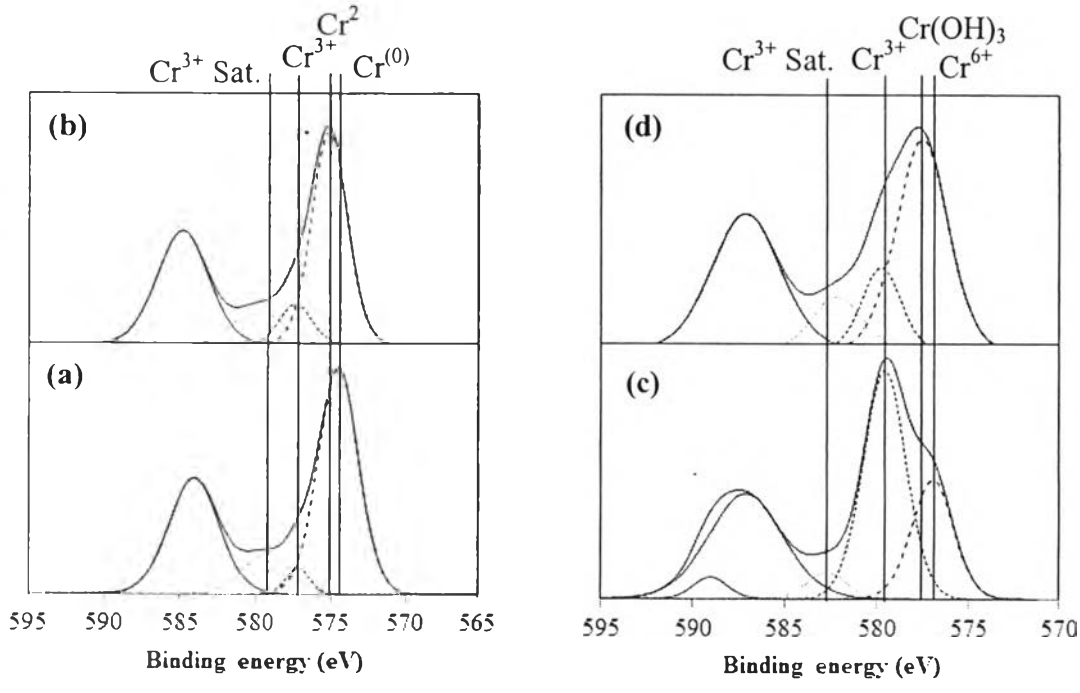

Figure 8.2 XPS spectra of (a) fresh Cr/Al_2O_3, (b) spent Cr/Al_2O_3, (c) fresh CrO_3/Al_2O_3, and (d) spent CrO_3/Al_2O_3.

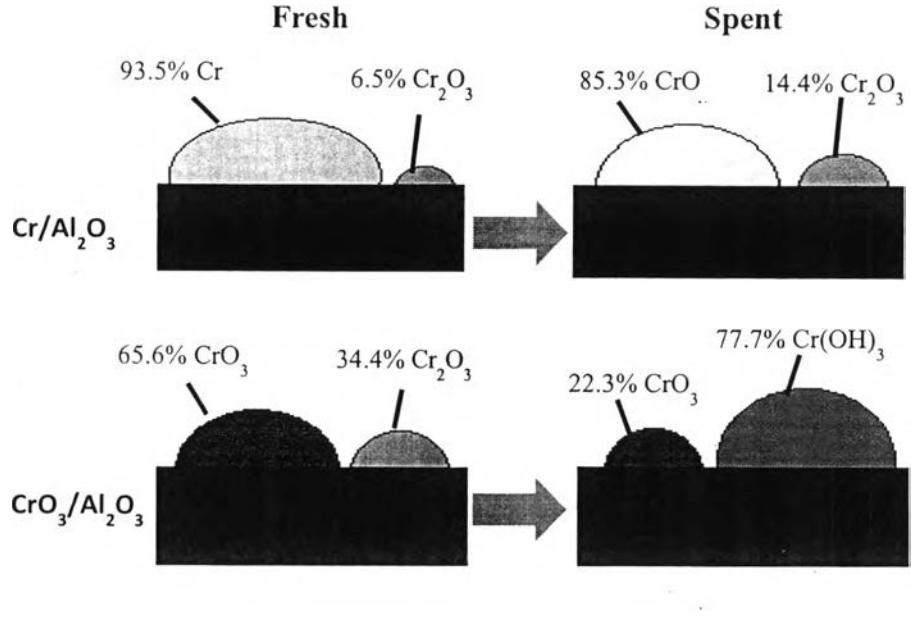

Figure 8.3 Surface composition of chromium-modified catalysts.

The XRD patterns are shown in Figure 8.1 in order to confirm the characteristic of alumina and the existence of metallic Cr and chromium oxide on alumina surface. The peak located at $2\theta = 67.5^{o}$ is the characteristic of gamma alumina (Liu *et al.*, 2012). Moreover, the peaks due to CrO_3 is observed at $2\theta = 31.2^{o}$ (Zhao *et al.*, 2008), and the peak due to metallic Cr is observed at $2\theta = 42.7^{o}$ (Castillejo *et al.*, 2014). As a result, it can be concluded that there is a formation of CrO_3 on alumina surface, and metallic Cr is present on the surface of the reduced catalyst.

Additionally, to further verify the chemical state of metallic Cr and CrO_3 over γ-alumina surface, XPS was employed. Figure 8.2 illustrates the XPS spectra of fresh and spent chromium catalysts. Moreover, Table 8.1 presents the binding energies (eV) and compositions of chromium species on γ-alumina surface. Figure 8.2 (a) displays the XPS spectrum of fresh metallic Cr/Al_2O_3 catalysts. The Cr $2p_{3/2}$ binding energies peaks of 574.5 and 576.1 eV are interpreted to metallic Cr (Eriksson *et al.*, 2002) and Cr_2O_3 (Biesinger *et al.*, 2011), accounting for 93.5% and 6.5%, respectively. In addition, the characteristic satellite peak of Cr^{3+} is located at 580.3 eV (Eriksson *et al.*, 2002). For the spent Cr/Al_2O_3, Figure 8.2 (b) shows that the Cr $2p_{3/2}$ binding energies of 575.2 and 576.4 eV are interpreted to CrO and Cr_2O_3 (Biesinger *et al.*, 2011), accounting for 85.3% and 14.7%, respectively. Furthermore, the binding energy peak of 580.6 eV is interpreted to the characteristic satellite of Cr^{3+} (Eriksson *et al.*, 2008). Figure 8.2 (C) displays the XPS spectrum of fresh CrO_3/Al_2O_3 catalyst. The Cr $2p_{3/2}$ binding energies of 576.9 and 579.6 eV are interpreted to Cr_2O_3 and CrO_3 (Biesinger *et al.*, 2011), accounting for 34.4% and 65.6%, respectively. Furthermore, the binding energy of 582.7 eV is represented to the characteristic satellite peak of Cr^{3+} (Eriksson *et al.*, 2008). For spent CrO_3/Al_2O_3 catalyst, the XPS spectrum are displayed in Figure 8.2 (d), the Cr $2p_{3/2}$ binding energies of 577.6 and 579.7 eV are interpreted to CrO_3 and $Cr(OH)_3$ (Biesinger *et al.*, 2011), accounting for 22.3% and 77.7%, respectively. Moreover, the characteristic satellite peak of Cr^{3+} is located at 582.2 eV (Eriksson *et al.*, 2008). As a result, it is found that the surface of Cr/Al_2O_3 catalyst is composed of metallic Cr more than 90%, and the rest is Cr_2O_3. On the other hand, after the catalytic testing, metallic Cr was entirely oxidized to CrO, and there are CrO and Cr_2O_3 formation on spent

Cr/Al_2O_3 catalyst. Moreover, Hoang *et al.*, (2000) explained that metallic Cr is easily to oxidize when exposed to the air and oxidizing agent. For fresh CrO_3/Al_2O_3 catalyst, there are formations of two species; that are, Cr_2O_3 and CrO. On the contrary, CrO_3 was entirely reduced to Cr^{3+}, and there is OH group formation on the metal oxide surface. Additionally, the increase in CO_2 formation in the gaseous product supports this evidence. $Cr(OH)_3$ is found after the catalytic testing due to the adsorption of ethanol over metal oxide surface, leaving OH group at the surface.

Table 8.2 Physical properties of Cr-modified catalysts

Catalyst	Surface Area $(m^3/g)^a$	Pore Volume $(cm^3/g)^a$	Pore Diameter $(nm)^b$
Al_2O_3	206.8	0.1792	49.31
Cr/Al_2O_3	170.3	0.1730	45.89
CrO_3/Al_2O_3	158.7	0.1677	30.23

[a] determined using BET method
[b] determined using B.J.H method

The BET surface area and pore volume decrease when chromium is loaded on alumina as shown in Table 8.2. The decreases in surface area and pore volume of catalyst prepared by using incipient wetness impregnation technique suggest that chromium solution were adsorbed deeply in the pore of alumina, resulting in the formation of chromium species inside the pores.

8.4.2 Catalytic Activity of Cr-modified Catalysts

The yield of oil, water, and gas obtained from the catalytic dehydration of bio-ethanol by using Al_2O_3, and Cr-modified catalysts are reported in Table 8.3. It is found that the yield of oil and water are decreased, compared to parent alumina. However, the gas yield is slightly increased from 76.3 wt% to 85.5 wt% and 88.3 wt% by using Cr/Al_2O_3 and CrO_3/Al_2O_3 catalysts. This indicates that both Cr/Al_2O_3 and CrO_3/Al_2O_3 catalysts give mostly gaseous product with a low amount of oil.

Table 8.3 Product yields obtained from using Cr-modified catalysts

Catalyst	% Yield			Conversion
	Oil	Water	Gas	
Non-catalyst	4.9	8.8	86.3	99.2
Al_2O_3	3.1	20.6	76.3	98.7
Cr/Al_2O_3	2.3	12.2	85.5	98.1
CrO_3/Al_2O_3	2.9	8.8	88.3	99.4

The gaseous products obtained from the catalytic dehydration of bio-ethanol by using Cr/Al_2O_3 and CrO_3/Al_2O_3 catalysts are shown in Figure 8.3. It is found that ethylene is found as a main component in the gaseous products. Moreover, the other gaseous co-products; that are methane, ethane, propylene, and butylene are present in a trace amount. On the other hand, the formations of metallic Cr and CrO_3 on alumina surface result in the suppression of ethylene formation. Additionally, the suppression of ethylene can be ranked in the order: $CrO_3/Al_2O_3 > Cr/Al_2O_3 > Al_2O_3$.

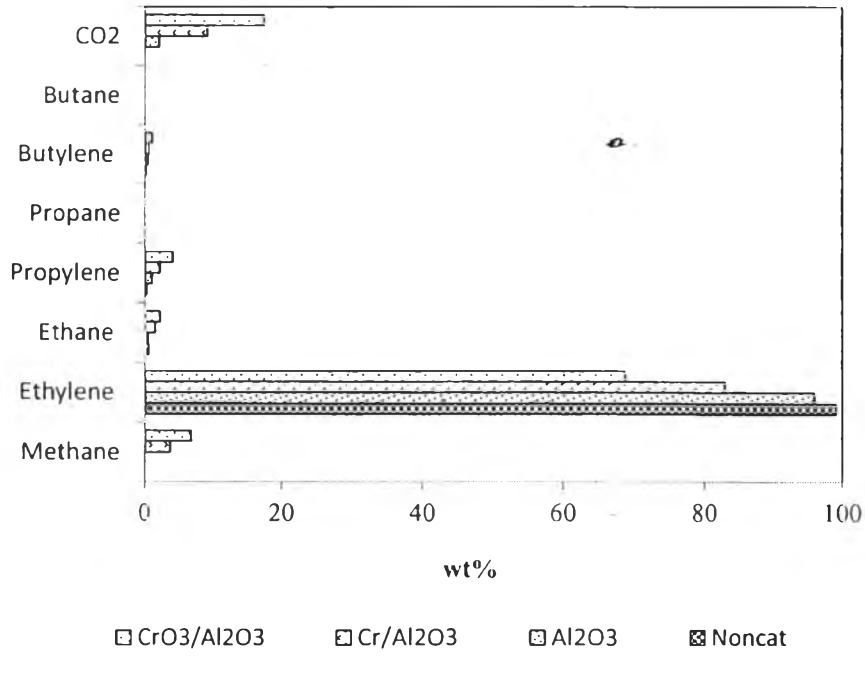

Figure 8.4 Gaseous product distributions from using Cr-modified alumina catalysts.

Table 8.4 Liquid product distribution obtained from using Cr catalysts

Catalyst	Product Distribution (wt%)	
	Oxygenates	Hydrocarbons
Non-catalyst	88.8	11.2
Al_2O_3	92.2	7.8
Cr/Al_2O_3	80.6	19.4
CrO_3/Al_2O_3	73.6	26.4

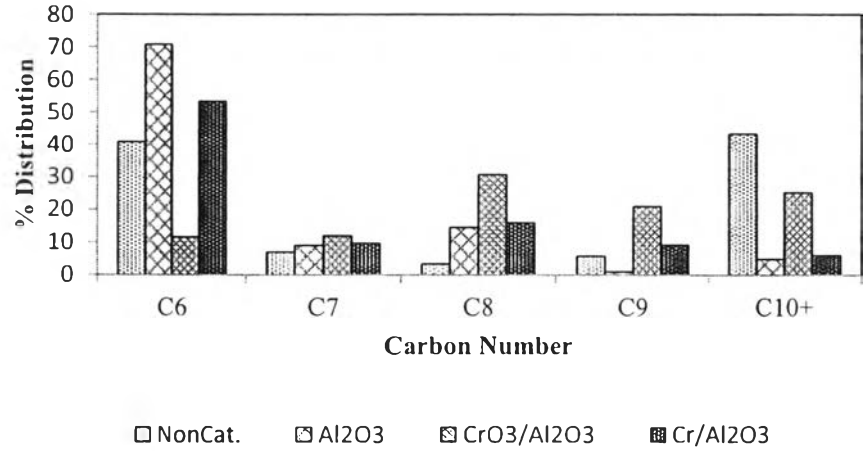

Figure 8.5 Carbon number distribution in oils from using Cr-modified catalysts.

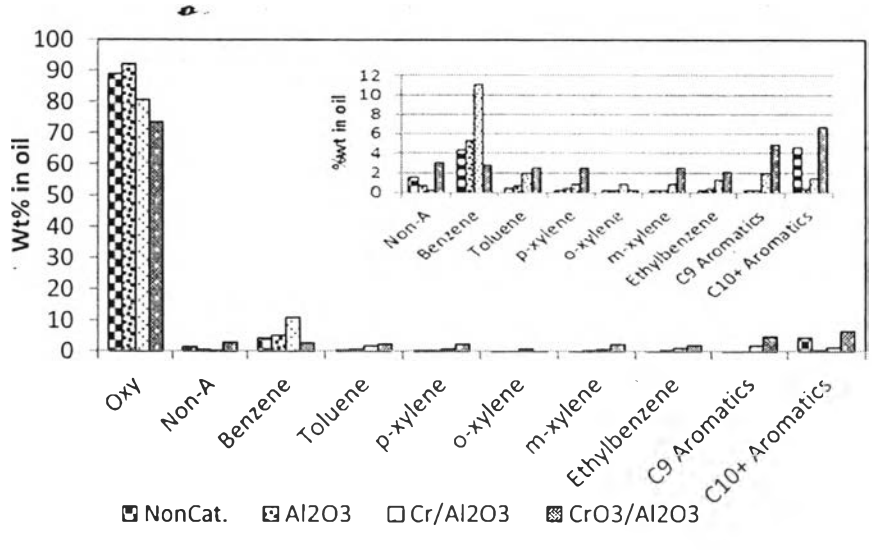

Figure 8.6 Liquid product distribution (wt%) from using Cr-modified catalysts.

In addition, the compositions of liquid products obtained from the catalytic dehydration of bio-ethanol are shown in Table 8.4. It is found that the liquid products are composed of oxygenate compounds and hydrocarbons. Compared to alumina, both Cr/Al_2O_3 and CrO_3/Al_2O_3 catalysts exhibit the decrease in oxygenate compounds with the increasing hydrocarbons. Moreover, the hydrocarbons are increased from 7.9 wt% to 19.7 wt% and 26.4 wt% by using Cr/Al_2O_3 and CrO_3/Al_2O_3 catalysts, respectively. This indicates that both Cr/Al_2O_3 and CrO_3/Al_2O_3 catalysts seem to enhance the formation of hydrocarbons. Moreover, the ability to produce hydrocarbons can be ranked in the order: CrO_3/Al_2O_3>Cr/Al_2O_3

Additionally, as seen from Table 8.4, the liquid products are composed of two main products; that are, oxygenate compounds and hydrocarbons. As a result, the hydrocarbons are enhanced by using both Cr/Al_2O_3 and CrO_3/Al_2O_3 catalysts, respectively. Figure 8.4 displays the carbon number distributions. It is found that most of hydrocarbons obtained from using Cr/Al_2O_3 catalyst are distributed in C_6 products of both non-aromatics and aromatics. However, CrO_3/Al_2O_3 catalyst exhibits the decreases in C_6 products, whereas the hydrocarbons in the range of C_7 to C_{10}+ are continuously increased as compared to pure Al_2O_3. This indicates that Cr/Al_2O_3 and CrO_3/Al_2O_3 catalysts have different ability to promote hydrocarbon formation. Figure 8.5 shows that the hydrocarbons are composed of non-aromatics, benzene, toluene, mixed-xylenes, C_9, and C_{10}+-aromatics. Additionally, the non-aromatics are composed of aliphatic and cyclic hydrocarbons. Moreover, 1,5-hexadiene and 1,3-cyclohexadiene are found as a main components in aliphatic and cyclic hydrocarbons, respectively. As a result, it can be explained that chromium catalysts of both metallic Cr and CrO_3 promote ethylene chain growth through oligomerization and cyclization, leading to 1,5-hexadiene and 1,3-cyclohexadiene formations, respectively. In addition, 1,3-cyclohexadiene can undergo dehydrogenation reaction, resulting in benzene formation. However, as seen in Figure 8.5, benzene is suppressed by using CrO_3/Al_2O_3 catalyst. This indicates that CrO_3/Al_2O_3 catalyst is able to promote further reactions of benzene, resulting in the increasing of all hydrocarbons larger than benzene, and the reaction pathways are shown in Figure 8.6.

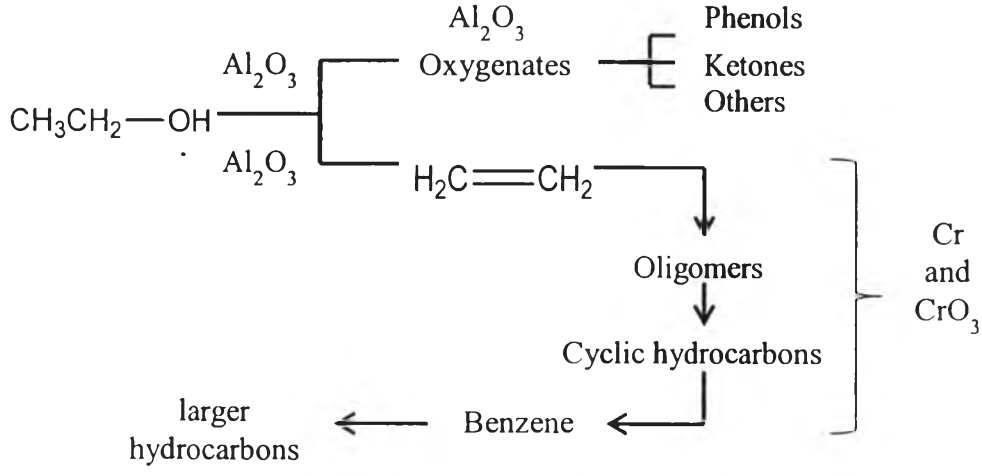

Figure 8.7 Ethanol transformation pathways using Cr-modified catalysts.

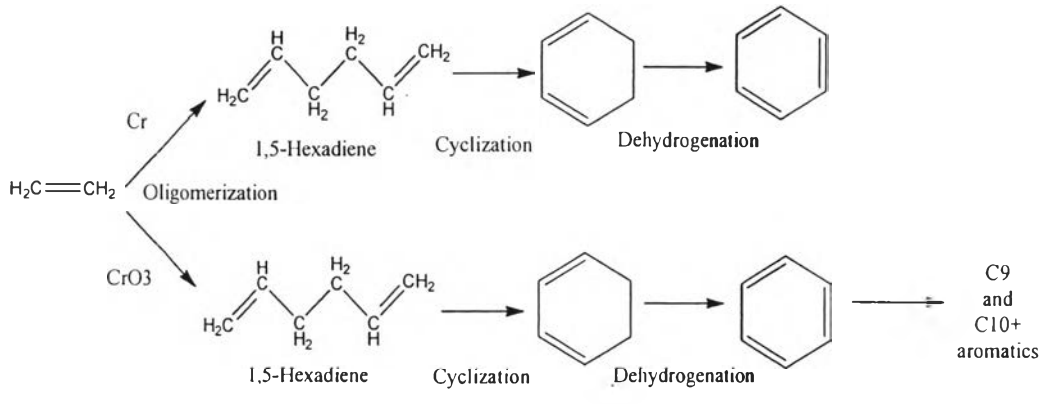

Figure 8.8 Ethylene chain growth using Cr-modified catalysts.

Table 8.5 Compositions of oxygenates (wt%) from using Cr-modified catalysts

Catalyst	Product Distribution (wt%)		
	Phenols	Ketones	Others
Non-catalyst	9.4	85.0	5.60
Al_2O_3	64.5	35.5	0.0
Cr/Al_2O_3	90.6	9.40	0.0
CrO_3/Al_2O_3	60.5	38.5	1.5

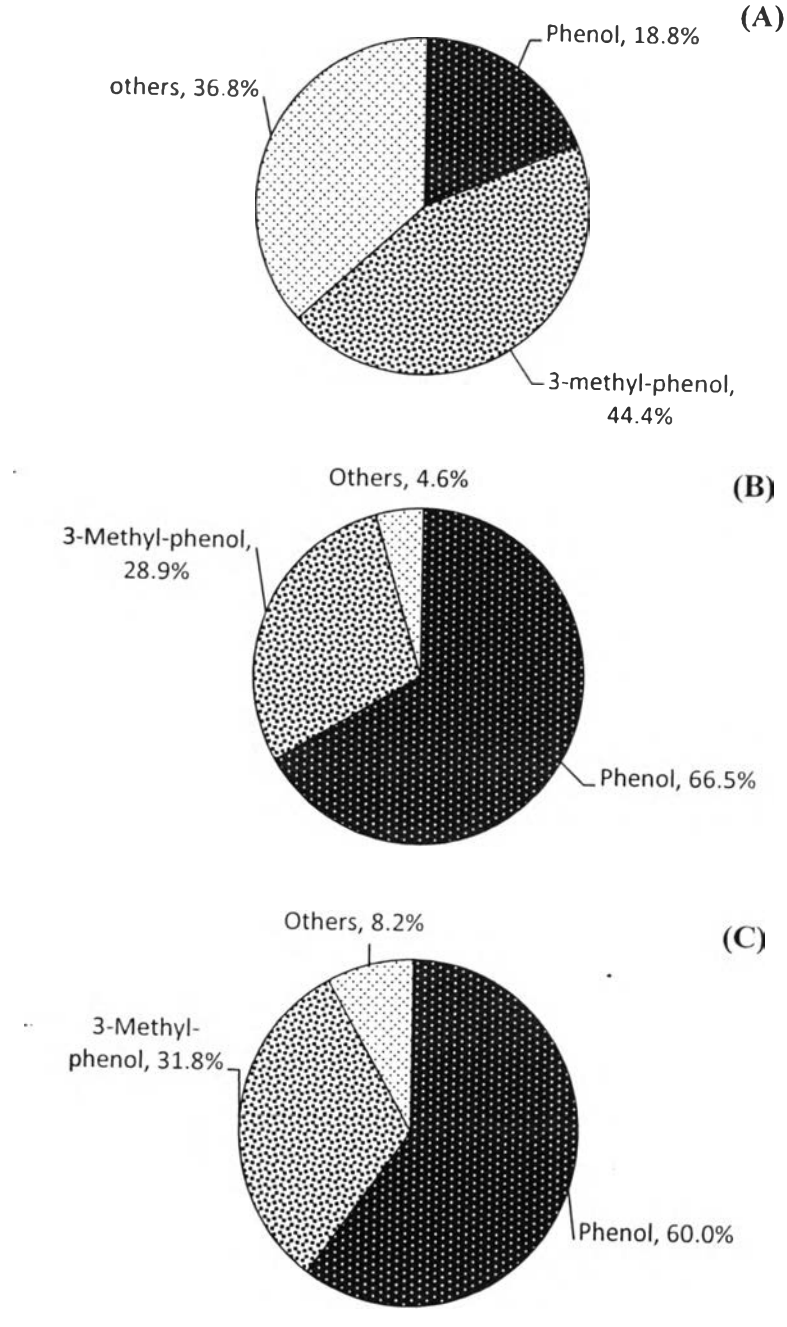

Figure 8.9 Compositions of phenols (wt%) found in liquid products: (A) Al_2O_3, **(B)** Cr/Al_2O_3, and (C) CrO_3/Al_2O_3.

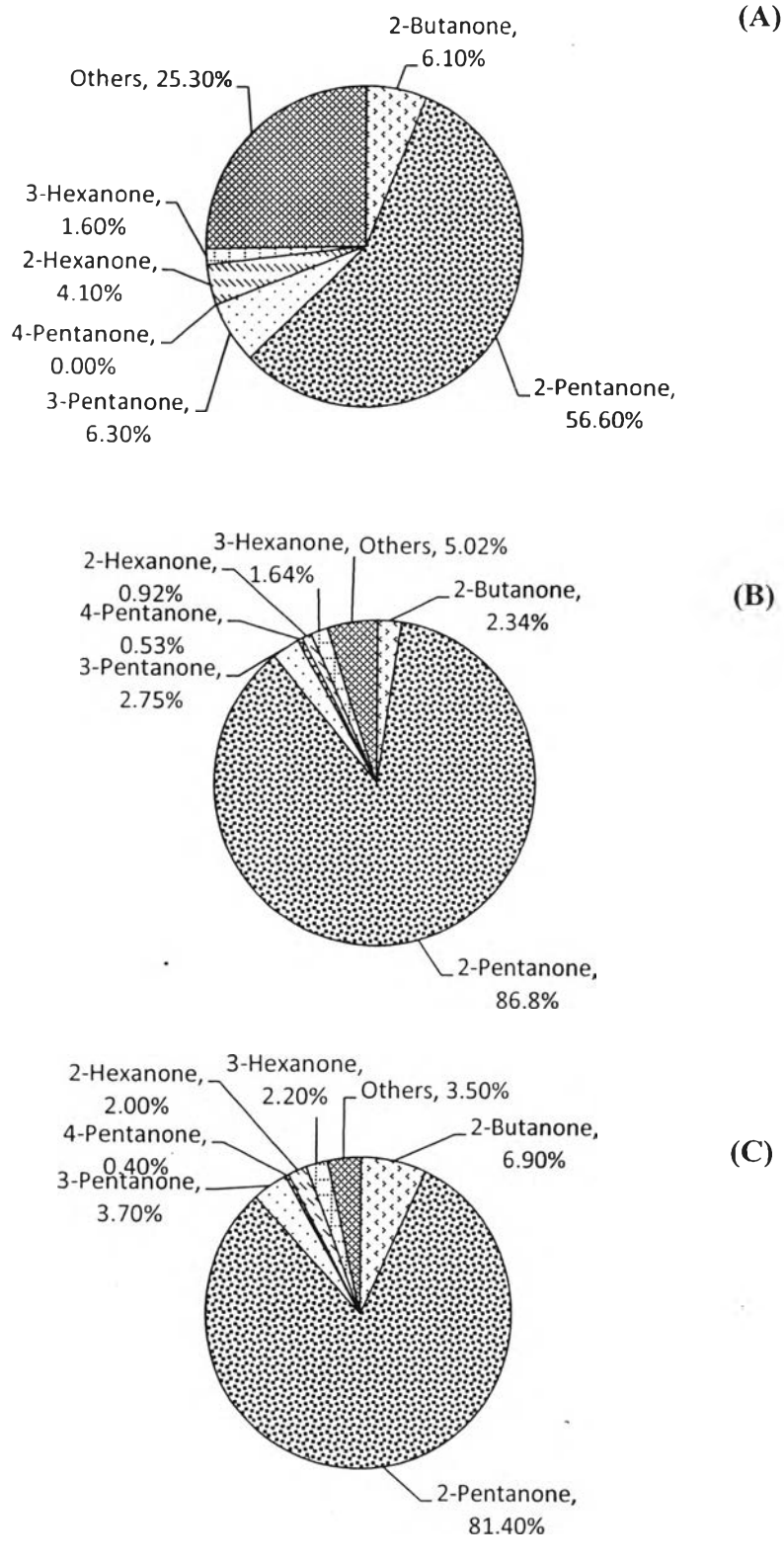

Figure 8.10 Compositions of ketones (wt%) found in liquid products: (A) Al_2O_3, (B) Cr/Al_2O_3, and (C) CrO_3/Al_2O_3.

8.4.3 Oxygenate Compounds Production

The oxygenate compounds are found as a main product in oil, and Table 8.5 presents the compositions of oxygenate compounds. It is found that there are two main components in oxygenate compounds; that are, phenol and ketones compounds. Moreover, the other is referred to a trace of ether compounds. From Table 8.5, it is observed that phenol compounds are significantly enhanced from 64.5 wt% to 90.6 wt% by using Cr/Al_2O_3, and ketone compounds are slightly increased from 35.5 wt% to 38.5 wt% using CrO_3/Al_2O_3 catalyst. From the results, it can be noticed that all catalysts give a high composition of oxygenate compounds, indicating that all catalyst might promote similar pathways of oxygenate compounds formation, and the compositions of phenol and ketone compounds are displayed in Figure 8.7 and 8.8, respectively. Among the oxygenate compounds, phenol compounds are found as a major component in oxygenate compounds for all catalysts. Compared to pure alumina, phenol is decreased in the order of: Cr/Al_2O_3 > CrO_3/Al_2O_3 > Al_2O_3. Additionally, ketone compounds are found as the second co-products in oxygenate compounds, and among ketone compounds, 2-pentanone is made dominantly. As a result, it is found that when compared to unmodified alumina, 2-pentanone is decreased from 81.4 wt% to 56.5 wt% by using Cr/Al_2O_3; however, it is increased to 86.8 wt% by using CrO_3/Al_2O_3. Therefore, 2-pentanone selectivity is decreased in the order: $CrO_3/Al_2O_3 \geq Al_2O_3 > Cr/Al_2O_3$.

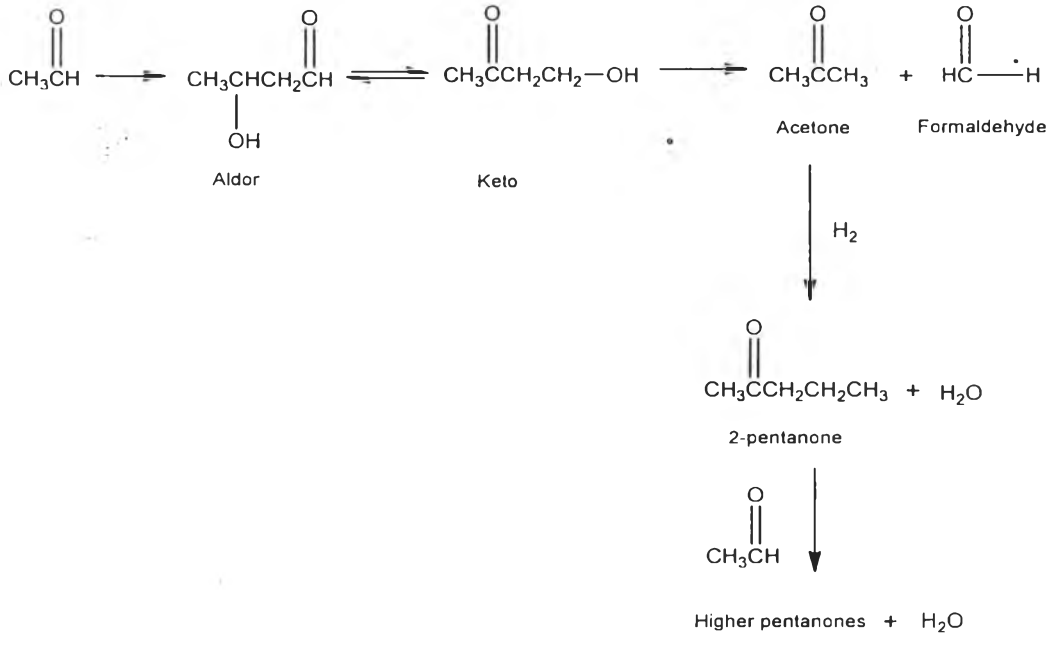

Figure 8.11 Reaction pathways of ethanol to oxygenate compounds (He *et al.*, 2005).

8.4.4 Effect of Oxidation State of Cr

Different oxidation states of chromium are investigated in the catalytic dehydration of bio-ethanol. From the result, it is found that both oxidation states; that are, metallic Cr and CrO_3, seem to promote similar pathways of ethanol transformation that leads to the increase in hydrocarbons. On the other hand, the ability to promote hydrocarbons is different, meaning that CrO_3/Al_2O_3 catalyst has higher ability than Cr/Al_2O_3 catalyst since they have different surface compositions. This can be explained by using the results of XPS analysis that there is a formation of OH group on chromium oxide surface after the catalytic testing. Krishmakumar et al., (2009) explained that a metal oxide containing OH group may act as Bronsted acid sites, helping to increase hydrocarbons in oil. Moreover, the formation of OH group on the metal oxide surface can be explained by the adsorption of ethanol on anion vacancy, which forms ethoxy group and leaves oxygen-hydrogen on the surface, leading to ethylene formation (Shinohara *et al.*, 1999). Additionally, both

Cr/Al_2O_3 and CrO_3/Al_2O_3 catalysts promote similar pathways of ethanol transformation; that are dehydration, oligomerization, and dehydrogenation, resulting in the increase in hydrocarbons. Even though the catalysts promote the same dominant reaction pathways, resulting in the increase of hydrocarbons, the oxygenate compounds still remain a major component in oily product. This indicates that the formation of oxygenate compounds are governed by Al_2O_3 support, and the pathways of oxygenate compounds formation are displayed in Figure 8.12.

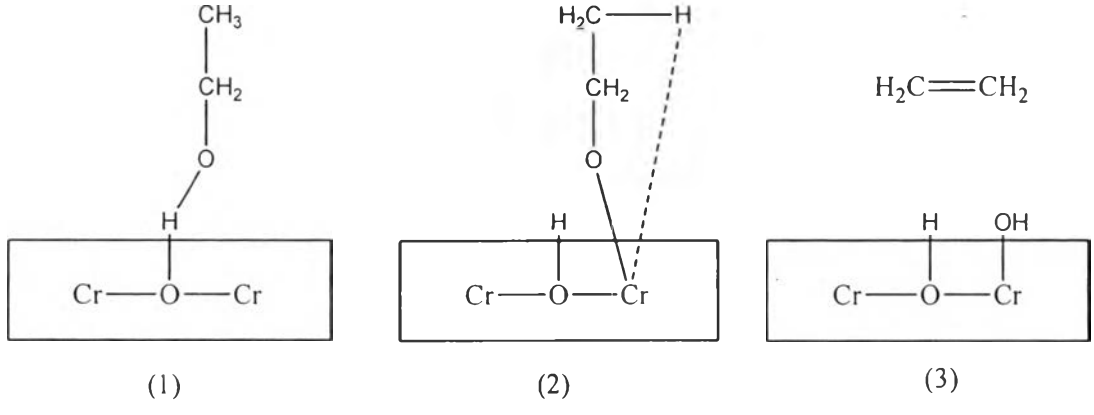

Figure 8.12 OH group formation over metal oxide surface (Shinohara *et al.*, 1999).

8.5 Conclusions

Chromium catalysts with different oxidation states were examined in the catalytic dehydration of bio-ethanol, aiming to investigate the effect of oxidation state on product distributions. From the result, it was revealed that both oxidation states of chromium promotes promoted similar pathways of ethanol transformation; that are, dehydration, oligomerization, cyclization, H-elimination, or dehydrogenation as dominant reactions, resulting in the increasing of hydrocarbon products in oil. Even though Cr-modified catalysts exhibited the increase in hydrocarbons, but they had different ability. As a result, it was found that CrO_3/Al_2O_3 catalyst displayed higher ability to produce hydrocarbons than metallic Cr/Al_2O_3 catalyst due to the new acid sites formation on the metal oxide surface. With using CrO_3/Al_2O_3 catalyst, the hydrocarbons were considerably enhanced, but

the oxygenate compounds were considerably suppressed. Moreover, the catalytic activity for producing hydrocarbons can be ranked in the order of CrO_3/Al_2O_3 > Cr/Al_2O_3 > Al_2O_3. The obtained hydrocarbons were composed of non-aromatics and aromatics. In addition, the non-aromatics consisted of aliphatic and cyclic hydrocarbons, meaning that Cr-modified catalysts might promote ethylene chain growth through olefins, unsaturated aliphatic, cyclic, and then aromatic hydrocarbons. Moreover, oxygenate compounds were composed of phenol and ketone products.

8.6 References

Aguado, J., Calleja, G., Carrero, A., and Moreno, J. (2008) One-step synthesis of chromium and aluminium containing SBA-15 materials: New phillips catalysts for ethylene polymerization. Chemical Engineering Journal, 137(2), 443-452.

Biesinger, M.C., Payne, B.P., Grosvenor, A.P., Lau, L.W.M., Gerson, A.R., and Smart, R.S.C. (2011) Resolving surface chemical states in XPS analysis of first row transition metals, oxides and hydroxides: Cr, Mn, Fe, Co and Ni. Applied Surface Science, 257(7), 2717-2730.

Calleja, G., Aguado, J., Carrero, A., and Moreno, J. (2005) Chromium supported onto swelled Al-MCM-41 materials: a promising catalysts family for ethylene polymerization. Catalysis Communications, 6(2), 153-157.

Castillejo, F.E., Marulanda, D.M., Olaya, J.J., and Alfonso, J.E. (2014) Wear and corrosion resistance of niobium–chromium carbide coatings on AISI D2 produced through TRD. Surface and Coatings Technology, 254, 104-111.

Chen, H., Liu, X., Hu, W., Ning, Y., and Jiang, T. (2007) Effects of halide in homogeneous Cr(III)/PNP/MAO catalytic systems for ethylene tetramerization toward 1-octene. Journal of Molecular Catalysis A: Chemical, 270(1–2), 273-277.

Eriksson, M., Sainio, J., and Lahtinen, J. (2002) Chromium deposition on ordered alumina films: An x-ray photoelectron spectroscopy study of the interaction with oxygen. The Journal of Chemical Physics, 116(9), 3870-3874.

He, D., Ding, Y., Chen, W., Lu, Y., and Luo, H. (2005) One-step synthesis of 2-pentanone from ethanol over K-Pd/MnOx-ZrO2-ZnO catalyst. Journal of Molecular Catalysis A: Chemical, 226(1), 89-92.

Hoang, D.L. and Lieske, H. (2000) Temperature-programmed reduction study of chromium oxide supported on zirconia and lanthana–zirconia. Thermochimica Acta, 345(1), 93-99.

Idriss, H. and Seebauer, E.G. (2000). Reactions of ethanol over metal oxides. Journal of Molecular Catalysis A: Chemical, 152(1–2), 201-212.

Krishnakumar, T., Jayaprakash, R., Pinna, N., Phani, A.R., Passacantando, M., and Santucci, S. (2009) Structural, optical and electrical characterization of antimony-substituted tin oxide nanoparticles. Journal of Physics and Chemistry of Solids, 70(6), 993-999.

Liu, C., Li, J., Zhang, Y., Chen, S., Zhu, J., and Liew, K. (2012) Fischer–Tropsch synthesis over cobalt catalysts supported on nanostructured alumina with various morphologies. Journal of Molecular Catalysis A: Chemical, 363–364, 335-342.

Shao, H., Li, Y., Gao, X., Cao, C., Tao, Y., Lin, J., and Jiang, T. (2014) Microporous zeolite supported $Cr(acac)_3$/PNP catalysts for ethylene tetramerization: Influence of supported patterns and confinement on reaction performance. Journal of Molecular Catalysis A: Chemical, 390, 152-158.

Shinohara, Y., Nakajima, T., and Suzuki, S. (1999) A theoretical study of the dehydration and the dehydrogenation processes of alcohols on metal oxides using MOPAC. Journal of Molecular Structure: THEOCHEM, 460(1–3), 231-244.

Speiser, F., Braunstein, P., and Saussine, L. (2005) Catalytic Ethylene Dimerization and Oligomerization: Recent Developments with Nickel Complexes Containing P,N-Chelating Ligands. Accounts of Chemical Research, 38(10), 784-793.

Sun, Y., Chen, Y., Mao, G., Ning, Y., and Jiang, T. (2014) Boron- and silicon-bridged bis(diphenylphosphino)-type ligands for chromium-catalyzed ethylene oligomerization. Chinese Science Bulletin, 59(21), 2613-2617.

Takahara, I., Saito, M., Matsuhashi, H., Inaba, M., and Murata, K. (2007) Increase in the number of acid sites of a H-ZSM5 zeolite during the dehydration of ethanol. Catalysis Letters, 113(3-4), 82-85.

Zhang, X., Wang, R., Yang, X., and Zhang, F. (2008) Comparison of four catalysts in the catalytic dehydration of ethanol to ethylene. Microporous and Mesoporous Materials, 116(1–3), 210-215.

Zhao, Q., Yuan, J.J., Wen, G.H., and Zou, G.T. (2008) Preparation and magnetoresistance of thin CrO2 films. Journal of Magnetism and Magnetic Materials, 320(19), 2356-2358.